Charged-Higgs effects in $B \to (D)\tau\nu$ decays

Stéphanie Trine
Institut für Theoretische Teilchenphysik, Universität Karlsruhe, D-76128 Karlsruhe, Germany

We update and compare the capabilities of the purely leptonic mode $B \to \tau\nu$ and the semileptonic mode $B \to D\tau\nu$ in the search for a charged Higgs boson.

I. INTRODUCTION

Supersymmetric extensions of the standard model (SM) – or more generally extensions that require the existence of at least one additional Higgs doublet – generate new flavour-changing interactions already at tree-level via the exchange of a charged Higgs boson. The coupling of H^+ to fermions grows with the fermion mass. It is thus natural to look at (semi)leptonic B decays with a τ in the final state to try to uncover this type of effects. In a two-Higgs-doublet-model (2HDM) of type II, where up-type quarks get their mass from one of the two Higgs doublets and down-type quarks from the other one, H^+ effects are entirely parametrized by the H^+ mass, M_H, and the ratio of the two Higgs vacuum expectation values, $\tan\beta = v_u/v_d$. They can compete with the exchange of a W^+ boson for large values of $\tan\beta$ [1]. In the minimal supersymmetric extension of the SM (MSSM), the tree-level type-II structure is spoilt by radiative corrections involving supersymmetry-breaking terms. The effective scalar coupling g_S then exhibits an additional dependence on sparticle mass parameters when $\tan\beta$ is large ($q = u, c$) [2, 3]:

$$H_{eff}^{H^+} = -2\sqrt{2} G_F V_{qb} \frac{m_b m_\tau}{M_B^2} g_S \left[\overline{q}_L b_R\right] \left[\overline{\tau}_R \nu_L\right] + h.c., \qquad g_S = \frac{M_B^2 \tan^2\beta}{M_H^2} \frac{1}{(1+\varepsilon_0 \tan\beta)(1+\varepsilon_\tau \tan\beta)}, \tag{1}$$

where $\varepsilon_{0,\tau}$ denote sparticle loop factors. The correction induced can be of order one. However, the access to the Higgs sector remains exceptionally clean. In Eq.(1), g_S has been normalized such that it gives the fraction of effects in the $B \to \tau\nu$ amplitude, which is very sensitive to H^+ exchange: $\mathcal{B}(B \to \tau\nu)/\mathcal{B}(B \to \tau\nu)^{SM} = |1 - g_S|^2$. The $B \to D\tau\nu$ channel is less sensitive (though better in this respect than other modes such as $B \to D^*\tau\nu$) but, as we will see, exhibits a number of features that make it, too, play an important part in the hunt for the charged Higgs boson.

II. $\mathcal{B}(B \to D\tau\nu)$ VERSUS $\mathcal{B}(B \to \tau\nu)$

The current capabilities of $\mathcal{B}(B \to D\tau\nu)$ and $\mathcal{B}(B \to \tau\nu)$ to constrain H^+ effects are compared in Fig.1 for $g_S \geq 0$ (as is typically the case in the MSSM or the 2HDM-II). The lower sensitivity of the $B \to D\tau\nu$ mode comes from the different momentum dependence of the Higgs contribution with respect to the longitudinal W^+ one[20]: $(d\Gamma(B \to D\tau\nu)/dq^2)^{W_\parallel^+ + H^+} \propto |1 - g_S(q^2/M_B^2)/(1 - m_c/m_b)|^2$ with $q \equiv p_B - p_D$. On the other hand, the theory prediction for $\mathcal{B}(B \to \tau\nu)$ suffers from large parametric uncertainties from the CKM matrix element V_{ub} and the B decay constant f_B. In contrast, V_{cb} is known with better than 2% accuracy from inclusive $B \to X_c \ell\nu$ ($\ell = e, \mu$) decays, $|V_{cb}| = (41.6 \pm 0.6) \times 10^{-3}$ [4], and the form factors $f_+(q^2)$ and $f_0(q^2)$ describing the $B \to D$ transition are very well under control, as we now discuss in more detail.

To this end, we introduce the following conformal transformation:

$$q^2 \to z(q^2, t_0) \equiv \frac{\sqrt{(M_B + M_D)^2 - q^2} - \sqrt{(M_B + M_D)^2 - t_0}}{\sqrt{(M_B + M_D)^2 - q^2} + \sqrt{(M_B + M_D)^2 - t_0}}, \tag{2}$$

which maps the complex q^2 plane, cut along $q^2 \geq (M_B + M_D)^2$, onto the disk $|z| < 1$. The form factors f_+ and f_0 are analytic in z in this domain, up to a few subthreshold poles, and can thus be written as a power series in z after these poles are factored out ($i = +, 0$) [10]:

$$f_i(q^2) = \frac{1}{P_i(q^2)\phi_i(q^2, t_0)} \left[a_0^i(t_0) + a_1^i(t_0) z(q^2, t_0) + \ldots\right], \tag{3}$$

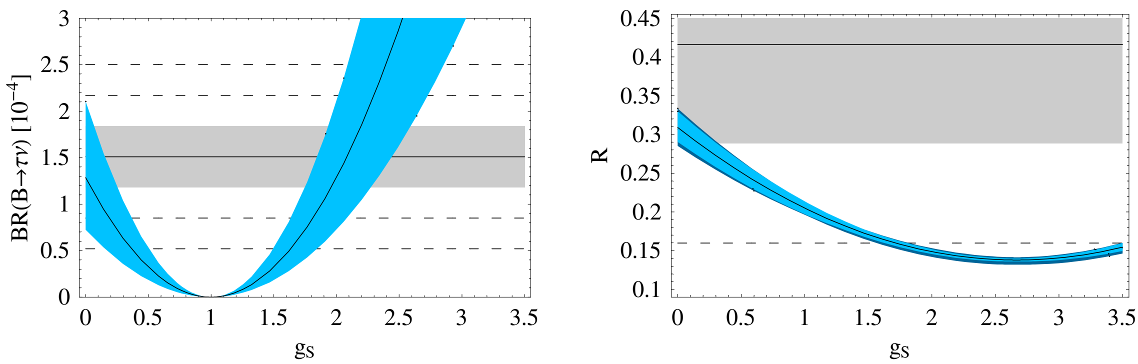

FIG. 1: Left: $\mathcal{B}(B \to \tau\nu)$ as a function of g_S. Light gray band: $\mathcal{B}^{\rm exp} = (1.51 \pm 0.33) \times 10^{-4}$ [5]. Gray (blue) band: $\mathcal{B}^{\rm th}$ for $|V_{ub}| = (3.95 \pm 0.35) \times 10^{-3}$ [4] and $f_B = 216 \pm 38\,\mathrm{MeV}$ [6] (in this last case, we add errors linearly to stay on the conservative side). Right: $R \equiv \mathcal{B}(B \to D\tau\nu)/\mathcal{B}(B \to D\ell\nu)$ as a function of g_S. Light gray band: $R^{\rm exp} = (41.6 \pm 11.7 \pm 5.2)\%$ [7]. Dark gray (dark blue) band: $R^{\rm th}$ with the HFAG vector form factor before ICHEP08 [8]. Gray (blue) band: $R^{\rm th}$ with the HFAG vector form factor after ICHEP08 [5]. The dashed lines indicate the 2 and 3-sigma limits. The ratio m_c/m_b in the $\overline{\rm MS}$ scheme has recently been determined with very high accuracy: $m_c/m_b = 0.2211 \pm 0.0044$ [9]. We inflated the error on this number and set $m_c/m_b = 0.22 \pm 0.01$ to reduce the discrepancy with the HFAG estimation [5].

where the function P_i gathers the pole singularities and an arbitrary analytic function ϕ_i can be factored out as well.

This parametrization has been used in Ref.[11] with the choice $t_0 = q^2_{\rm max} = (M_B - M_D)^2$, together with heavy-quark spin symmetry inputs, to derive the following ansatz for the vector form factor:

$$f_+(q^2) \equiv \frac{M_B + M_D}{2\sqrt{M_D M_B}} V_1(q^2), \quad V_1(q^2) = \mathcal{G}(1)\left[1 - 8\rho^2 z(q^2,t_0) + (51\rho^2 - 10) z(q^2,t_0)^2 - (252\rho^2 - 84) z(q^2,t_0)^3\right], \quad (4)$$

where V_1 is defined such that it reduces to the Isgur-Wise function in the heavy-quark limit and $\mathcal{G}(1) \equiv V_1(q^2_{\rm max})$. The parameters $|V_{cb}|\mathcal{G}(1)$ and ρ^2 can be determined from $B \to D\ell\nu$ experimental data. Before this summer, the HFAG averages [8] based on BELLE, CLEO, and ALEPH data read: $|V_{cb}|\mathcal{G}(1) = (42.3 \pm 4.5) \times 10^{-3}$ and $\rho^2 = 1.17 \pm 0.18$ (with a $|V_{cb}|\mathcal{G}(1)$-ρ^2 correlation of 0.93). The recent BABAR results [12] and [13] have now been included, leading to a substantial improvement [5]: $|V_{cb}|\mathcal{G}(1) = (42.4 \pm 0.7 \pm 1.4) \times 10^{-3}$ and $\rho^2 = 1.19 \pm 0.04 \pm 0.04$ (with $|V_{cb}|\mathcal{G}(1)$-ρ^2 correlation 0.88). The old and new vector form factors are compared in Fig.2 (left), where we have defined as usual $w = (M_B^2 + M_D^2 - q^2)/(2M_B M_D)$.

For the scalar form factor, we adopt the ansatz of Ref.[14]:

$$f_0(q^2) \equiv \frac{(w+1)\sqrt{M_D M_B}}{M_B + M_D} S_1(q^2) = \frac{1}{z(q^2, M_1^2) z(q^2, M_2^2) \phi_0(q^2, t_0)} \left[a_0^0(t_0) + a_1^0(t_0)\, z(q^2,t_0)\right], \quad (5)$$

where $t_0 = (M_B + M_D)^2 \left(1 - \sqrt{1 - (M_B - M_D)^2/(M_B + M_D)^2}\right)$ such that $|z|_{\rm max}$ is minimized, $M_1 = 6.700\,\mathrm{GeV}$ and $M_2 = 7.108\,\mathrm{GeV}$ [15] are the subthreshold poles, and ϕ_0 is obtained from Eq.(10) of Ref.[14] setting $Q^2 = 0$ and $\eta = 2$:

$$\phi_0(q^2, t_0) = \sqrt{\frac{2(M_B^2 - M_D^2)^2}{16\pi}} \frac{\sqrt{(M_B + M_D)^2 - q^2}}{((M_B + M_D)^2 - t_0)^{1/4}} \frac{z(q^2,0)^2}{(q^2)^2} \left(\frac{z(q^2,t_0)}{t_0 - q^2}\right)^{-1/2} \left(\frac{z(q^2,(M_B - M_D)^2)}{(M_B - M_D)^2 - q^2}\right)^{-1/4}. \quad (6)$$

Following [16], we truncate the series (3) after the first two terms. This is motivated by the fact that $|z|_{\rm max} = 0.032$ and that a similar parametrization for f_+, when fitted to experimental data, produces the same result as Eq.(4) in very good approximation [16]. Then, $|V_{cb}|a_0^0(t_0)$ and $|V_{cb}|a_1^0(t_0)$ are determined imposing the conditions (i) $|V_{cb}|S_1(0) = |V_{cb}|V_1(0)$ and (ii) $|V_{cb}|S_1(q^2_{\rm max}) = (4.24 \pm 0.27)\%$ (corresponding to $|V_{cb}| = (41.6 \pm 0.6) \times 10^{-3}$ from $B \to X_c\ell\nu$ [4] and $S_1(q^2_{\rm max}) = 1.02 \pm 0.05$ from HQET [16]). The scalar form factors obtained in this way from the old and new $|V_{cb}|V_1$ are not very different, as one can see on Fig.2 (right).

The recent progress on $|V_{cb}|V_1$ allows to reduce the errors on the SM predictions for the two $B \to D\tau\nu$ branching fractions: $\mathcal{B}(B^- \to D^0\tau^-\bar{\nu})^{SM} = \left(0.70^{+0.06}_{-0.05}\right)\%$, $\mathcal{B}(\bar{B}^0 \to D^+\tau^-\bar{\nu})^{SM} = \left(0.65^{+0.06}_{-0.05}\right)\%$ (differing essentially due to

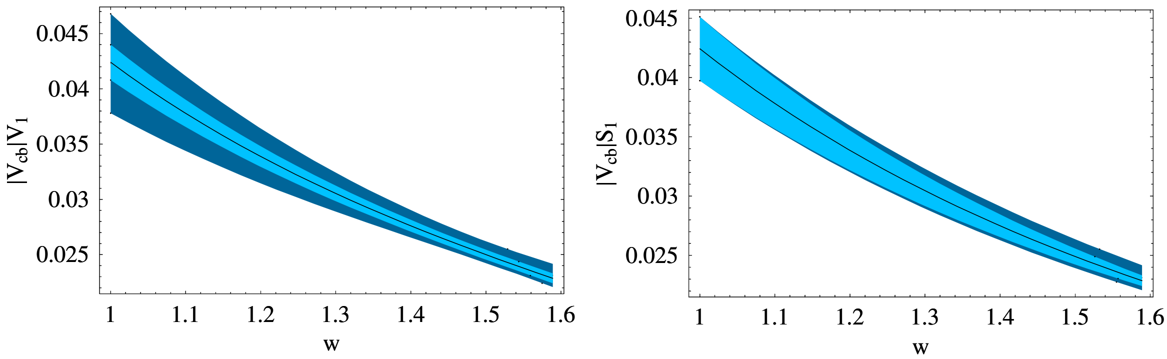

FIG. 2: Vector (left) and scalar (right) form factors corresponding to the $|V_{cb}|\mathcal{G}(1)$ and ρ^2 determinations of HFAG before (dark gray/dark blue)[8] and after (gray/blue)[5] ICHEP08. With the new determination, the errors on $|V_{cb}|V_1$ and $|V_{cb}|S_1$ are smaller than 4% and 7%, respectively.

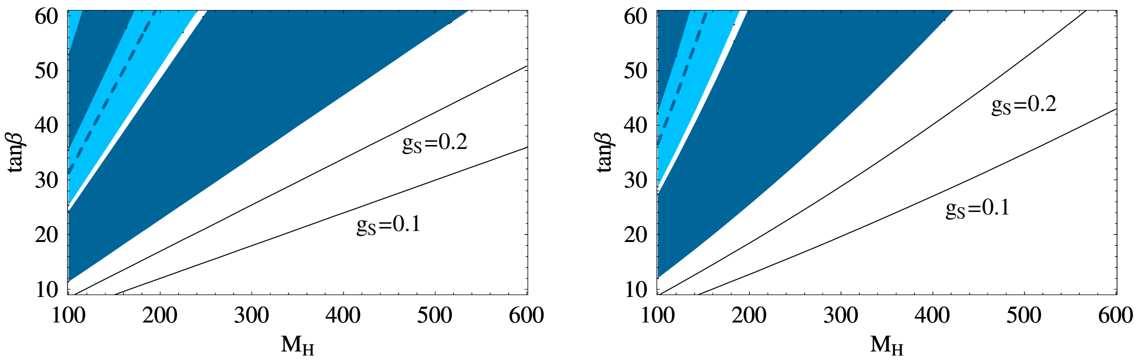

FIG. 3: 95% C.L. exclusion zones in the $(M_H, \tan\beta)$ plane from $\mathcal{B}(B \to \tau\nu)$ (dark gray/dark blue) and R (gray/blue) in a 2HDM (left) and in the MSSM with $\varepsilon_0 = 0.01$ and $\varepsilon_\tau \simeq 0$ (right). The exclusion limits are directly read from the gray (blue) bands in Fig.1. They differ from those usually found in the literature in that experimental and theory errors are not simply added in quadrature and the dependence of the errors on the H^+ contribution is taken into account.

$\tau_{B^0} \neq \tau_{B^+}$). The errors from $|V_{cb}|V_1$, however, already cancel to a large extent in the ratio $R \equiv \mathcal{B}(B \to D\tau\nu)/\mathcal{B}(B \to D\ell\nu)$, which is why the nice improvement in Fig.2 has little impact on Fig.1 (right), already dominated by the error on $S_1(q^2_{\max})$: $R^{SM} = 0.31 \pm 0.02$. This estimation is compatible with the one obtained from lattice methods: $R^{SM}_{latt} = 0.28 \pm 0.02$ [17]. Note that replacing condition (ii) by a constraint on $S_1(q^2_{\max})/V_1(q^2_{\max})$ from HQET would lead to a similar error on R. Still, an interesting 95% C.L. bound on g_S can already be obtained from R: $g_S < 1.79$, complementary to the bounds from $\mathcal{B}(B \to \tau\nu)$: $g_S < 0.36 \,\cup\, 1.64 < g_S < 2.73$. The corresponding exclusion zones in the $(M_H, \tan\beta)$ plane are depicted in Fig.3. The error assigned to $S_1(q^2_{\max})$ is quite conservative, so the above constraints are robust. At the three-sigma level, it is not possible to extract any interesting bound from R yet, but its experimental knowledge is expected to improve in the near future. Its role to constrain H^+ effects will then of course depend on the new central value. For the moment, a 15% measurement with the same central value would exclude $g_S > 0.29$ at the 95% C.L..

III. $B \to D\tau\nu$ DIFFERENTIAL DISTRIBUTIONS

If a hint for a charged Higgs boson is seen at the branching fraction level, $B \to D\tau\nu$ has a great advantage over $B \to \tau\nu$: it allows to analyze the same data points on a differential basis, better suited to discriminate between effective scalar-type interactions and other effects. The $d\Gamma(B \to D\tau\nu)/dq^2$ distribution, in particular, has already been studied in great detail [18]. The polarization of the τ is also known as a H^+ analyzer [19], yet it requires the

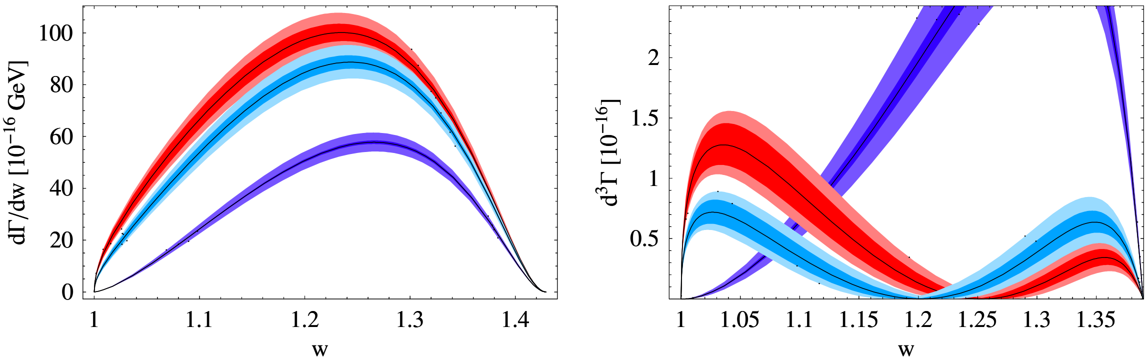

FIG. 4: $d\Gamma(B \to D\tau\nu)/dw$ (left) and $d\Gamma(B \to D\nu\tau[\to \pi\nu])/dE_\pi d\cos\theta_{D\pi} dw$ with $E_\pi = 1.8\,\text{GeV}$ and $\cos\theta_{D\pi} = -1$ (right) for $g_S = 0$ (gray/red), $g_S = 0.35$ (light gray/light blue), and $g_S = 1.75$ (dark gray/dark blue). These values are still allowed by $\mathcal{B}(B \to D\tau\nu)$ and $\mathcal{B}(B \to \tau\nu)$ at the 95% C.L.. The various curves have been obtained using the more recent HFAG vector form factor [5]. The lighter bands take all errors into account, while the darker bands only take into account the error on $S_1(q^2_{\text{max}})$. One could of course also normalize the above differential distributions to $d\Gamma(B \to D\ell\nu)/dw$ to reduce the impact of the errors on f_+.

knowledge of the τ momentum, which cannot be accessed at B factories as the τ does not travel far enough for a displaced vertex and decays into at least one more neutrino.

A straightforward way to nevertheless exploit the sensitivity of the τ polarization to H^+ effects and at the same time retain the information from the q^2 spectrum is to look at the subsequent decay of the τ into a pion and a neutrino [16]. The direction of the pion is indeed directly correlated with the polarization of the τ. Integrating over the neutrino momenta, we end up with a triple differential decay distribution $d\Gamma(B \to D\nu\tau[\to \pi\nu])/dq^2 dE_\pi d\cos\theta_{D\pi}$. An explicit formula is given in Eqs.(9-11) of Ref.[16] (with $F_V \equiv f_+$ and $F_S \equiv f_0$). Its sensitivity to g_S is illustrated in Fig.4 for $E_\pi = 1.8\,\text{GeV}$ and $\cos\theta_{D\pi} = -1$. For comparison, we also display the q^2 spectra corresponding to the same g_S values. Of course, in practice, one should not fix E_π or $\theta_{D\pi}$, but rather perform a (unbinned) maximum likelihood fit of the triple differential decay distribution to the available data points. The information from the q^2 spectrum in the dominant $\tau \to \ell\nu\bar{\nu}$ decay channel should also be included in the fit to make the most out of experimental data.

IV. CONCLUSION

The form factors $f_+(q^2)$ and $f_0(q^2)$ in the $B \to D\tau\nu$ transition are under good control. As a result, the ratio $R \equiv \mathcal{B}(B \to D\tau\nu)/\mathcal{B}(B \to D\ell\nu)$ can be predicted with 7% accuracy in the SM: $R^{SM} = 0.31 \pm 0.02$, where the 5% uncertainty on the scalar form factor at zero recoil $S_1(q^2_{\text{max}})$ is the main error source. This allows to derive useful constraints on the effective H^+ coupling g_S. Together with the constraints from $\mathcal{B}(B \to \tau\nu)$, we obtain: $g_S < 0.36 \;\cup\; 1.64 < g_S < 1.79$, i.e., the window around $g_S = 2$ left over by $\mathcal{B}(B \to \tau\nu)$ is now nearly completely excluded by R alone. These bounds should be strengthened soon thanks to the current considerable experimental efforts on both modes. In this respect, one should pay particular attention to the $B \to D\tau\nu$ differential distributions as these are especially well-suited to discriminate between effective scalar interactions and other types of effects and, if the former are seen, to extract the coupling g_S with good precision.

Acknowledgments

It's a pleasure to thank my collaborators Ulrich Nierste and Susanne Westhoff. Discussions with Matthias Steinhauser about the ratio m_c/m_b and with Christoph Schwanda and Laurenz Widhalm about experimental issues are also warmly acknowledged. Work supported by the DFG grant No. NI 1105/1-1, by the DFG-SFB/TR9, and by the

EU contract No. MRTN-CT-2006-035482 (FLAVIAnet).

---

[1] W. Hou, Phys. Rev. **D48**, 2342 (1993).

[2] M. S. Carena, D. Garcia, U. Nierste and C. E. M. Wagner, Nucl. Phys. **B577**, 88 (2000); A. J. Buras, P. H. Chankowski, J. Rosiek and L. Slawianowska, Nucl. Phys. **B659**, 3 (2003); A. Akeroyd and S. Recksiegel, J. Phys. G **29**, 2311 (2003); H. Itoh, S. Komine and Y. Okada, Prog. Theor. Phys. **114**, 179 (2005).

[3] For a recent global phenomenological analysis, see for example D. Eriksson, F. Mahmoudi and O. Stal, arXiv:0808.3551 [hep-ph].

[4] C. Amsler *et al.* (Particle Data Group), Phys. Lett. **B667**, 1 (2008).

[5] Heavy Flavor Averaging Group, update after ICHEP08, http://www.slac.stanford.edu/xorg/hfag/.

[6] A. Gray *et al.* (HPQCD Collaboration), Phys. Rev. Lett. **95**, 212001 (2005).

[7] B. Aubert *et al.* (BABAR Collaboration), Phys. Rev. Lett. **100**, 021801 (2008).

[8] Heavy Flavor Averaging Group, arXiv:0808.1297 [hep-ex].

[9] K. Chetyrkin, J. Kühn and M. Steinhauser, Comput. Phys. Commun. **133**, 43 (2000). Input values: J. Kühn, M. Steinhauser and C. Sturm, Nucl. Phys. **B778**, 192 (2007).

[10] See for example the discussion by F. J. Yndurain, arXiv:hep-ph/0212282.

[11] I. Caprini, L. Lellouch and M. Neubert, Nucl. Phys. **B530**, 153 (1998). See also the earlier related works: C. Bourrely, B. Machet and E. de Rafael, Nucl. Phys. **B189**, 157 (1981); C.G. Boyd, B. Grinstein and R.F. Lebed, Phys. Rev. **D56**, 6895 (1997).

[12] B. Aubert *et al.* (BABAR Collaboration), these proceedings, arXiv:0807.4978 [hep-ex].

[13] B. Aubert *et al.* (BABAR Collaboration), arXiv:0809.0828 [hep-ex].

[14] R. Hill, arXiv:hep-ph/0606023.

[15] E. Eichten and C. Quigg, Phys. Rev. **D49**, 5845 (1994).

[16] U. Nierste, S. Trine and S. Westhoff, Phys. Rev. **D78**, 015006 (2008), arXiv:0801.4938 [hep-ph].

[17] J.F. Kamenik and F. Mescia, Phys. Rev. **D78**, 014003 (2008), arXiv:0802.3790[hep-ph].

[18] B. Grzadkowski and W. Hou, Phys. Lett. **B283**, 427 (1992); K. Kiers and A. Soni, Phys. Rev. **D56**, 5786 (1997).

[19] J. Kalinowski, Phys. Lett. **B245**, 201 (1990); D. Atwood, G. Eilam and A. Soni, Phys. Rev. Lett. **71**, 492 (1993); Y. Grossman and Z. Ligeti,Phys. Lett. **B332**, 373 (1994); M. Tanaka, Z. Phys. **C67**, 321 (1995); R. Garisto, Phys. Rev. **D51**, 1107 (1995); G. H. Wu, K. Kiers and J. N. Ng, Phys. Rev. **D56**, 5413 (1997).

[20] Note that the latter, though helicity-suppressed, is still (slightly) larger than the transverse W^+ contribution for all q^2 values.